Eur. Phys. J. Special Topics **227**, 2349–2360 (2019)
© EDP Sciences, Springer-Verlag GmbH Germany, part of Springer Nature, 2019
https://doi.org/10.1140/epjst/e2018-800059-9

THE EUROPEAN PHYSICAL JOURNAL SPECIAL TOPICS

Regular Article

Multiscale cyclic dynamics in light harvesting complex in presence of vibrations and noise

Shmuel Gurvitz[1,2,a], Gennady P. Berman[3], and Richard T. Sayre[4]

[1] Department of Particle Physics and Astrophysics, Weizmann Institute, 76100 Rehovot, Israel
[2] Center for Nonlinear Studies, Los Alamos National Laboratory, Los Alamos, NM 87545, USA
[3] Theoretical Division, T-4, Los Alamos National Laboratory, Los Alamos, NM 87545, USA
[4] New Mexico Consortium, Los Alamos, NM 87544, USA

Received 15 April 2018 / Received in final form 5 July 2018
Published online 18 January 2019

Abstract. Starting from the many-body Schrödinger equation, we derive a new type of Lindblad master equations describing a cyclic exciton/electron dynamics in the light harvesting complex and the reaction center. These equations resemble the master equations for the electric current in mesoscopic systems, and they go beyond the single-exciton description by accounting for the multi-exciton states accumulated in the antenna, as well as the charge-separation, fluorescence and photo-absorption. Although these effects take place on very different timescales, their inclusion is necessary for a consistent description of the exciton dynamics. Our approach reproduces both coherent and incoherent dynamics of exciton motion along the antenna in the presence of vibrational modes and noise. We applied our results to evaluate energy (exciton) and fluorescent currents as functions of sunlight intensity.

1 Introduction

The energy transfer in the light-harvesting complex (LHC) takes place via exciton propagation among pigments bound to the LHC proteins [1]. The exciton is created by resonant photo-absorption in an antenna pigment, leading to electron excitation from the ground to the excited energy level, $\gamma + E_0 \to E_1$, Figure 1. Due to the dipole–dipole interaction, V, the exciton then propagates between neighboring pigments to the reaction center (RC), while all excited and unexcited sites of the antenna remain neutral. Finally, the exciton arrives at the site N (the "donor" of the RC), where the primary charge separation occurs. The donor becomes positively charged, and the electron participates in chemical reactions in the RC. Finally, the donor is neutralized (reduced) by an electron ultimately arriving from water splitting, Figure 1, and at some time, τ, the cycle is completed.

[a] e-mail: shmuel.gurvitz@weizmann.ac.il

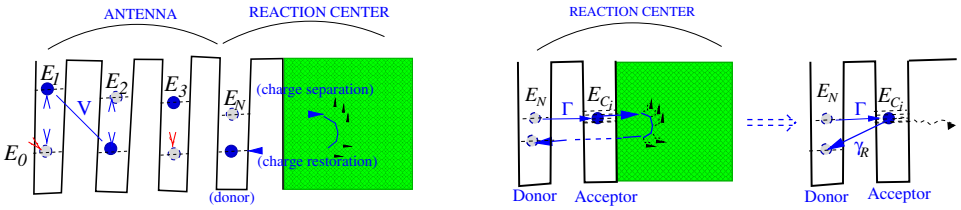

Fig. 1. Left: schematic picture of the electron cycle. The cycle is completed with restoration of the donor's neutrality (reduction). Right: the cycle is modeled by electron relaxation to the donor's ground state, through emission of the energy (fictitious boson) to the RC.

The dynamics of the exciton transfer along the antenna, including the primary charge separation, is very rapid (∼ps). Otherwise, the exciton would be lost by fluorescence or by other (recombination) processes, taking place on the time-scale of ∼ ns. In comparison, the duration of entire cycle (τ), completed with reduction of the oxidized primary electron donor, is much longer ($\sim \mu$s). During the charge separation stage, no excitons occupy the RC donor. However, they can be accumulated by the antenna pigments, and finally being lost by fluorescence, as shown schematically in Figure 1 (left panel). Usually, at normal light intensity, the study of energy-transfer in the LHC is limited by a single-exciton migration along the antenna pigment bed. At the same time, the research exists which goes beyond a single-exciton approach and which takes into account a cyclic regime and the multi-scale exciton dynamics in the LHCs (see, for instance, Refs. [2,3]). However, the *consistent* quantum-mechanical consideration of the exciton-electron cyclic regime in antenna-RC, which includes: (i) photo-absorption, (ii) fluorescence in antenna, (iii) charge restoration of the RC donor and (iv) both coherent and incoherent exciton-electron dynamics, does not exist. This is mainly because all these effects occur at significantly different time-scales, and require the development of adequate quantum-mechanical mathematical approaches. Indeed, without a consistent accounting of all these multi-scale processes, in the frames of quantum consideration, one cannot fully understand and describe the exciton dynamics in the LHC [1]. In particular, it is related to accumulation of one or more excitons inside the antenna with increase of the light intensity. These "trapped" excitons can damage the photosynthetic apparatus through de-excitation pathways leading to generation of oxygen singlets and other damaging products.

At first sight, exciton transport along the LHC looks similar to spinless electron transport in a mesoscopic system. Indeed, no more than one exciton can reside on the same site, if only one excitation is allowed for each site (hard exciton model) [4]. As a result, the exciton propagation along the antenna would be similar to electron tunneling through coupled-dot system. The treatment of electron current through the coupled dots can be greatly simplified by reducing the many-body Schrödinger equation to the Lindblad-type particle-number-resolved master equations [5–8]. It is desirable to realize this analogy and derive similar master equations for the exciton transport in the LHC, Figure 1. However, in this case we have to include restoration of the primary donor's neutrality, Figure 1 (right panel), since a similar cycle dynamics is not considered in electron transport through coupled-dot systems.

Thus, the charge separation is effectively accounted for by coupling the donor's level E_N to the acceptor, represented by a band of dense levels, E_{C_i} (sink), as displayed in right panel of Figure 1. This results in irreversible tunneling of the electron from the donor to the sink with a rate, $\Gamma \sim 1$/ps. In order to describe the effect of restoration of the donor's neutrality on the LHC dynamics, it is not necessary to know all details of the slow chemical reactions in the RC, initiated by the electrons. What is relevant is a period of the cycle (τ). Therefore, for our purposes, the RC can

be considered as a "Black Box", absorbing the donor electron of the energy, E_N, and then emitting it (by time τ) to the same donor site, but with a different energy, E_0.

This process can be modeled as a direct relaxation of an electron from the acceptor to the donor ground state, accompanied by emission of the energy $(E_N - E_0)$ to the RC. Although the cycle is completed by an electron coming from a different source (such as water splitting in the Photosystem II, etc.), its origin is not important for the exciton dynamics in the LHC, in particular, since all electrons are indistinguishable. To account this relaxation phenomenologically we add a fictitious field (bosonic bath) to the sink Hamiltonian, weakly coupled with all acceptor levels (E_{C_i}). If the bath is initially empty, the electron would exponentially decay to the donor's ground state with a relaxation decay rate, $\gamma_R = 1/\tau$, by emitting fictitious bosons with energy, $E_N - E_0$, as displayed in Figure 1 (right panel).

By modeling the energy transfer to the RC via quantized fictitious field, together with a quantized field, describing the light source and fluorescence, allows us to derive closed master equations for exciton dynamics in a complete quantum mechanical way. As a result, we would be able to evaluate the energy (exciton) current and the fluorescent current as functions of the incoming sunlight intensity, and also the probability of single and multi-exciton states inside the antenna. This approach can be considered as a framework for the treatment of the energy transfer through any network in the antenna complex and also in the presence of vibrations and noise.

The paper is organized as follows. In Sections 2 and 3, we describe the master equation for the photo-absorption by a single excitonic site, as well as primary charge separation and restoration on the donor site by using our wave-function approach. Section 4 deals with the general case of an N-site antenna with a detailed example of the two-site antenna. Section 5 includes an account of the vibrational modes and the related dichotomic noise, generated by the environment. Last section is the summary.

2 Rate equations for photo-absorption

In order to understand a general structure and origin of the particle-resolved master equations (presented in Sect. 4), describing the cyclic dynamics of the LHC, and conditions, at which these equations can be justified, we consider separately the exciton creation on the peripheral site and its decay to the RC from the inner site of the LHC.

Let us start from the photo-absorption on the first site, Figure 1 (left panel), separated from the rest of antenna. The corresponding Hamiltonian, H_1, can be written as,

$$H_1 = E_0 \hat{a}_0^\dagger \hat{a}_0 + E_1 \hat{a}_1^\dagger \hat{a}_1 + \sum_k \omega_k \hat{C}_k^\dagger \hat{C}_k + \sum_k \left(g_k \hat{B}_1^\dagger \hat{C}_k + H.c. \right), \tag{1}$$

where $\hat{a}_1^\dagger(\hat{a}_1)$ is an electron creation (annihilation) operator for the excited state, E_1, and $\hat{a}_0^\dagger(\hat{a}_0)$ is the same for the ground state, E_0, (in following we take $E_0 = 0$), while $\hat{C}_k^\dagger(\hat{C}_k)$ is a photon creation (annihilation) operator. $\hat{B}_1^\dagger = \hat{a}_1^\dagger \hat{a}_0$ denotes an exciton creation operator. The last term in (1) describes the electron–photon interaction in the rotating-wave approximation.

Using a similar technique, as for derivation of the particle-resolved rate equations for electron transport through multi-dot systems [8], we arrive to the following particle number-resolved master equations of a form,

$$\dot{\sigma}_{00}^{(p)}(t) = -\Gamma_{\text{in}} \sigma_{00}^{(p)}(t) + \Gamma_{\text{out}} \sigma_{11}^{(p-1)}(t), \tag{2a}$$

$$\dot{\sigma}_{11}^{(p)}(t) = \Gamma_{\rm in}\sigma_{00}^{(p)}(t) - \Gamma_{\rm out}\sigma_{11}^{(p)}(t), \tag{2b}$$

where $\sigma_{00}^{(p)}(t)$ and $\sigma_{11}^{(p)}(t)$ are probabilities of finding the electron in the ground state (E_0) and in the excited state (E_1), Figure 1, with p photons emitted by time t. Respectively, $\sigma_{\alpha\alpha}(t) = \sum_p \sigma_{\alpha\alpha}^{(p)}$, where $\alpha = 0, 1$, are total probabilities ($\sigma_{00}(t) + \sigma_{11}(t) = 1$). Here, $\Gamma_{\rm in}$ and $\Gamma_{\rm out}$ are rates of a photo-absorption, leading to electron transition from the ground to the excited state (exciton creation), and of a photo-emission in a reverse process (exciton annihilation). We found that $\Gamma_{\rm in} = \bar{n}\gamma$ and $\Gamma_{\rm out} = (\bar{n}+1)\gamma$, where $\bar{n} = n(E_1)$ is a number of photons with energy E_1 (which we call below the "light intensity") and $\gamma = 2\pi g^2(E_1)\rho(E_1)$, with ρ being density of photon states.

It follows from our derivation that the validity of equations (2) is based on Markovian approximation [9] (band-width is larger than γ). In this case, the contribution from the Green's function poles dominates in the equation of motion, leading to equations (2). However, if the band-width is very narrow (less than γ), these equations have to be modified. This problem will be discussed in a separate publication.

Equations (2) are identical to those describing the electron transport from the source to the drain through a single quantum dot, with $\Gamma_{\rm in}$ and $\Gamma_{\rm out}$ corresponding to the incoming and outgoing electron rates [5–8]. Summing up these equations over p and taking into account that $\sigma_{11}(t) = 1 - \sigma_{00}(t)$, one easily finds the following rate equation for $\sigma_{00}(t)$ which can be rewritten as a single equation,

$$\dot{\sigma}_{00}(t) = -(2\bar{n}+1)\gamma\sigma_{00}(t) + (\bar{n}+1)\gamma. \tag{3}$$

In the steady state limit, $\dot{\sigma}_{00}(t \to \infty) \to 0$, so the ground state occupation, $\bar{\sigma}_{00} = \sigma_{00}(t \to \infty)$ is $\bar{\sigma}_{00} = (\bar{n}+1)/(2\bar{n}+1)$. If the photon bath is in the thermal equilibrium state, then $\bar{n} = 1/(e^{E_1/T} - 1)$. As a result, the occupation of the ground state is $\bar{\sigma}_{00} = 1/(1 + e^{-E_1/T})$, which is a quite known result [10].

3 Primary charge separation and restoration by emission of energy

Consider the site N ("RC donor") of antenna, coupled to "acceptor", represented as a sink with dense levels, E_{C_i}, Figure 1 (right panel). As a result, an electron, occupying the excited level (E_N) of the RC donor, tunnels to the "acceptor", leaving the donor positively charged (primary charge separation). This process is very fast (∼ps) in a comparison with the time-scales of the subsequent chemical reactions in the RC (∼ μs). The cycle is completed when the positively charged site, N, is neutralized (reduced) by an electron. This is modeled by a direct relaxation of the electron from the acceptor band, E_{C_i}, to the donor's ground state with emission of energy $E_N - E_0$ to the RC. The latter is represented by emission of a fictitious boson, carrying this energy. In order to describe these processes quantum-mechanically, we introduce an effective Hamiltonian, H_N, for the donor, N, Figure 1 (right panel)

$$H_N = E_N\hat{a}_N^\dagger\hat{a}_N + \sum_i E_{C_i}\hat{a}_{C_i}^\dagger\hat{a}_{C_i} + \sum_p \bar{\omega}_p\hat{F}_p^\dagger\hat{F}_p + \sum_i\left(\tilde{V}_i\hat{a}_{C_i}^\dagger\hat{a}_N + \sum_p f_{ip}\hat{a}_0^\dagger\hat{a}_{C_i}\hat{F}_p^\dagger + H.c.\right). \tag{4}$$

Here, $\hat{a}_N^\dagger$ and $\hat{a}_{C_i}^\dagger$ denote electron creation operators at the site, N, and at a sub-level (i) of the acceptor, C. Respectively, $\hat{a}_0^\dagger \equiv \hat{a}_{0N}^\dagger$ is an electron creation operator at the ground state of the donor (we chose $E_0 \equiv E_{0N} = 0$). The operator, $\hat{F}_p^\dagger$, describes a

creation of fictitious bosons, bearing the energy transferred to the RC, and $\tilde{V}_i$ is a tunneling coupling between the donor, E_N, with the sub-level, E_{C_i}, of the acceptor, and f_{ip} is a coupling of an electron on the acceptor with fictitious bosons.

Consider the one-electron cycle, completed with emission of one fictitious boson, displayed in right panel of Figure 1. The wave function, describing a whole system (electron and fictitious bosons), can be written as,

$$|\Psi(t)\rangle = \left[b_N(t)\hat{a}_N^\dagger a_0 + \sum_i b_{C_i}(t)\hat{a}_{C_i}^\dagger \hat{a}_0 + \sum_p b_{0p}(t)\hat{F}_p^\dagger\right]|\bar{0}\rangle, \tag{5}$$

where $|\bar{0}\rangle \equiv \hat{a}_0^\dagger|0\rangle$ is the initial ("vacuum") state of the system, corresponding to empty boson bath and the electron, occupying the donor's ground state.

Substituting equation (5) into the Schrödinger equation, $i\partial_t|\Psi(t)\rangle = H_N|\Psi(t)\rangle$, we find the system of coupled equations for the amplitudes $b(t)$ with the initial conditions: $b_N(0) = 1$ and $b_{C_i}(0) = b_{0p}(0) = 0$. Using the same technique as in reference [8], we convert these equations to the following master equations for the density matrix of the system, $\sigma_{NN}(t) = |b_N(t)|^2$, $\sigma_{CC}(t) = \sum_i |b_{C_i}(t)|^2$, $\sigma_{00}(t) = \sum_p |b_{0p}(t)|^2$,

$$\dot{\sigma}_{NN}(t) = -\Gamma\sigma_{NN}(t), \tag{6a}$$
$$\dot{\sigma}_{CC}(t) = \Gamma\sigma_{NN}(t) - \gamma_R\sigma_{CC}(t), \tag{6b}$$
$$\dot{\sigma}_{00}(t) = \gamma_R\sigma_{CC}(t)\,, \tag{6c}$$

where $\Gamma = 2\pi|\tilde{V}|^2\rho_C$ is the charge-separation rate and $\gamma_R = (2\pi)^2|f|^2\rho_C\bar{\rho}\Delta = 1/\tau$ is the rate of an entire cycle, with ρ_C and $\bar{\rho}$ being the density of states of the acceptor sink and the bosonic bath, correspondingly. Here, $\Delta \simeq \Gamma$ is a width of the electron distribution on the acceptor. Both rates are phenomenological parameters, which are determined experimentally ($1/\Gamma \sim$ps and $1/\gamma_R \sim \mu$s-ms).

4 Exciton transport in N-site antenna

4.1 Master equations in general case

Now we extend our treatment on the N-site antenna chain, coupled with the electromagnetic field, describing photo-absorption and fluorescence, and with fictitious boson bath, describing the donor charge restoration, Figure 1. The total Hamiltonian, describing this system, is a combination of equations (1), (4), and it can be written as,

$$\mathcal{H}_N = \sum_k \omega_k \hat{C}_k^\dagger \hat{C}_k + \sum_{m=1}^{N} E_m \hat{B}_m^\dagger \hat{B}_m + \sum_i E_{C_i}\hat{a}_{C_i}^\dagger \hat{a}_{C_i} + \sum_p \bar{\omega}_p \hat{F}_p^\dagger \hat{F}_p + H_{\text{int}}, \tag{7}$$

where $\hat{B}_m^\dagger = \hat{a}_m^\dagger \hat{a}_{0m}$ is an exciton creation operator on the site m. Here too we assume that the ground state energy for all sites $m = 1, \ldots N$ is zero. All notations are the same as in equations (1), (4). The interaction term can be written as,

$$H_{\text{int}} = \sum_{m=1}^{N}\sum_k g_k \hat{B}_m^\dagger \hat{C}_k + \sum_{m=1}^{N-1} V_m \hat{B}_{m+1}^\dagger \hat{B}_m + \sum_i \left(\tilde{V}_i \hat{a}_{C_i}^\dagger \hat{a}_N + \sum_p f_{ip}\hat{a}_0^\dagger \hat{a}_{C_i}\hat{F}_p^\dagger\right) + H.c.$$

Here, the electromagnetic field is coupled with all sites of antenna. However, excitons can be generated only on the first antenna site, $m = 1$, by photon absorption. All

other sites, $m = 2, \dots N$, are coupled with the empty photon reservoirs. Thus, the excitons occupying these sites can only decay by the fluorescence.

Note that the exciton commutation relations [4], $[\hat{B}_m, \hat{B}_n^\dagger] = \delta_{mn}(1 - 2\hat{B}_m^\dagger \hat{B}_n)$, guarantee that two or more excitons cannot occupy the same site. Therefore, the exciton motion along the antenna, describing by the Hamiltonian (7), is similar to that of the spinless electron transport trough the coupled quantum dots. The corresponding master equation of the Lindblad-type can be derived from the time-dependent multi-particle Schrödinger equation, as discussed in previous examples. It represents a natural extension of equations (2) and (6), and can be written as (see Eq. (75) of Ref. [8]):

$$\dot{\sigma}_{\alpha\alpha'}^{(\nu,\ell)} = i\big(\mathcal{E}_{\alpha'} - \mathcal{E}_{\alpha}\big)\sigma_{\alpha\alpha'}^{(\nu,\ell)} + i\sum\nolimits_{\beta}\Big(\sigma_{\alpha\beta}^{(\nu,\ell)} V_{\beta\to\alpha'} - V_{\beta\to\alpha}\sigma_{\beta\alpha'}^{(\nu,\ell)}\Big) \\ -\tfrac{1}{2}\sigma_{\alpha\alpha'}^{(\nu,\ell)}\sum\nolimits_{\beta}(\Gamma_{\alpha\to\beta} + \Gamma_{\alpha'\to\beta}) + \sum\nolimits_{\beta,\beta'}\sigma_{\beta\beta'}^{(\nu',\ell')}\Gamma_{\beta\to\alpha,\beta'\to\alpha'}, \qquad (8)$$

where $|\alpha\rangle$, $|\beta\rangle$ enumerate all *discrete* multi-exciton states in the occupation number representation, and $\mathcal{E}_\alpha = \sum_{m\in\alpha} E_m$ is a total energy of the state, $|\alpha\rangle$. The upper indices, ν and ℓ, in the density matrix, $\sigma_{\alpha\alpha'}^{(\nu,\ell)}(t)$, denote the numbers of fluorescent photons and fictitious bosons emitted at time, t. Note that in the last ("gain") term, $(\nu', \ell') = (\nu - 1, \ell)$ or $(\nu', \ell') = (\nu, \ell - 1)$, whenever emission of fluorescence photons or fictitious bosons takes place (cf. with Eqs. (2)).

The second term in equation (8) describes the direct exciton transitions between neighboring sites, $V_{\beta\alpha} = V_{m,m+1} \equiv V_m$, via the dipole–dipole interaction. One can realize that the first and second terms of equation (8) represent the commutator of the density matrix with the Hamiltonian in the Lindblad equation [11]. The remaining two terms represent loss and gain processes generated by: (a) coupling of the site (1) to photon bath with rates $\Gamma_{\alpha,\beta} \equiv \Gamma_{\text{in,out}}$, equations (2), and all other sites with the rate $\Gamma_{\alpha,\beta} \equiv \gamma$; (b) charge separation with subsequent emission of fictitious bosons, leading to restoration of the donor's neutrality, with the rates $\Gamma_{\alpha,\beta} \equiv \Gamma, \gamma_R$, respectively, equations (6).

By solving equation (8), we can determine probabilities of any multi-exciton occupations, as well as the fluorescent current (in energy units), $I_{\text{fl}}(t)$, and the current of energy, $I_{\text{en}}(t)$, transferred to the RC. Those are given by (cf. with Refs. [5–8]),

$$I_{\text{en}}(t) = E_N \sum_{\nu,\ell}\sum_{\alpha_N} \ell\dot{\sigma}_{\alpha_N\alpha_N}^{(\nu,\ell)}(t) = E_N\gamma_R \sum_{\alpha_N}\sigma_{\alpha_N\alpha_N}(t),$$
$$I_{\text{fl}}(t) = \sum_{\nu,\ell}\sum_{m=2}^{N}\sum_{\alpha_m} E_m\nu\dot{\sigma}_{\alpha_m\alpha_m}^{(\nu,\ell)}(t) = \gamma\sum_{m=2}^{N}\sum_{\alpha_m} E_m\sigma_{\alpha_m\alpha_m}(t), \qquad (9)$$

where the index α_m enumerates all multi-exciton states containing the site m, and $\sigma_{\alpha_m\alpha_m}(t) = \sum_{\nu,\ell}\sigma_{\alpha_m\alpha_m}^{(\nu,\ell)}(t)$ is a corresponding occupation of these states, obtained from equation (8). Note that the first antenna site, where an exciton is created, is excluded from the fluorescent current, equation (9). Respectively, the total fluorescent current is $I_{\text{flT}}(t) = I_{\text{fl}}(t) + \Gamma_{\text{out}}E_1\sum_{\alpha_1}\sigma_{\alpha_1\alpha_1}(t)$, where $\Gamma_{\text{out}} = (\bar{n}+1)\gamma$, equation (2).

4.2 Two-site antenna

As an example for application of equation (8), we consider exciton transport through the two-site antenna, $(N = 2)$. First, we need to enumerate all possible exciton states of the system, $\{\alpha, \beta\} = \{0, 1 \dots, 5\}$. These are shown in Figure 2. Note that the

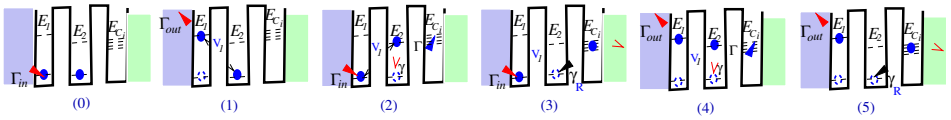

Fig. 2. Exciton states of the two-site antenna. All allowed exciton transitions for each states are indicated.

exciton propagates coherently between the sites (1) and (2) due to the dipole–dipole interaction, V_1. All other transitions are incoherent, where the related transition rates are shown for each of states.

Now we can rewrite explicitly the master equation (8) for the reduced density-matrix, $\sigma_{\alpha\alpha'} \equiv \sigma_{\alpha\alpha'}(t) = \sum_{\nu,\ell} \sigma^{(\nu,\ell)}_{\alpha\alpha'}(t)$, as

$$\dot\sigma_{00} = -\Gamma_{\rm in}\sigma_{00} + \Gamma_{\rm out}\sigma_{11} + \gamma\sigma_{22} + \gamma_R\sigma_{33}, \tag{10a}$$
$$\dot\sigma_{11} = iV_1(\sigma_{12} - \sigma_{21}) - \Gamma_{\rm out}\sigma_{11} + \Gamma_{\rm in}\sigma_{00} + \gamma\,\sigma_{44} + \gamma_R\sigma_{55}, \tag{10b}$$
$$\dot\sigma_{22} = iV_1(\sigma_{21} - \sigma_{12}) - (\gamma + \Gamma + \Gamma_{\rm in})\sigma_{22} + \Gamma_{\rm out}\sigma_{44}, \tag{10c}$$
$$\dot\sigma_{33} = -(\Gamma_{\rm in} + \gamma_R)\sigma_{33} + \Gamma_{\rm out}\sigma_{55} + \Gamma\sigma_{22}, \tag{10d}$$
$$\dot\sigma_{44} = -(\gamma + \Gamma_{\rm out} + \Gamma)\sigma_{44} + \Gamma_{\rm in}\sigma_{22}, \tag{10e}$$
$$\dot\sigma_{55} = -(\Gamma_{\rm out} + \gamma_R)\sigma_{55} + \Gamma_{\rm in}\sigma_{33} + \Gamma\sigma_{44}, \tag{10f}$$
$$\dot\sigma_{12} = i(E_2 - E_1)\sigma_{12} + iV_1(\sigma_{11} - \sigma_{22}) - (\Gamma_T/2)\sigma_{12}\,, \tag{10g}$$

where $\Gamma_T = \Gamma + \gamma + \Gamma_{\rm in} + \Gamma_{\rm out}$. One can easily verify that these equations display the probability conservation, $\sum_{\alpha=0}^{5}\sigma_{\alpha\alpha}(t) = 1$. Therefore, it is useful to replace one of equations (10a)–(10f) by the probability conservation.

By solving equations (10), we find the energy (exciton) current to the RC, equation (9),

$$I_{\rm en}(t) = \gamma_R E_2[\sigma_{33}(t) + \sigma_{55}(t)], \tag{11}$$

whereas the fluorescent current (from the second site, Fig. 2) and the total fluorescent current are given by,

$$I_{\rm fl}(t) = \gamma E_2[\sigma_{22}(t) + \sigma_{44}(t)]\,,$$
$$I_{\rm flT}(t) = I_{\rm fl}(t) + \Gamma_{\rm out}E_1[\sigma_{11}(t) + \sigma_{44}(t) + \sigma_{55}(t)]\,. \tag{12}$$

Consider now the steady-state limit, $t \to \infty$. Since in this limit $\dot\sigma_{\alpha\alpha'} \to 0$, equations (10) become a system of algebraic equations for $\bar\sigma \equiv \sigma(t \to \infty)$, which can be easily solved. The corresponding steady-state energy and fluorescent currents, equations (11), (12), are shown in Figure 3 as functions of the light intensity ($\bar n$). Note that $\bar n\gamma = \Gamma_{\rm in}$, equation (2), is a number of photons absorbed by the first site per unit time. Here, we chose for illustrative examples some generic values of parameters, not necessary related to a specific system, namely, γ=1/ns (fluorescent rate), $\gamma_R = 1/\tau = 10^{-3}\gamma = 1/\mu$s (charge restoration rate), $V_1 = 10^3\gamma$=1/ps (dipole–dipole coupling between sites), and $\Gamma = 10^3\gamma$=1/ps (charge separation rate). The exciton energy levels of all sites are taken the same, $E_1 = E_2 = \bar E$.

The steady-state energy current to the RC, $\bar I_{\rm en}$ (solid line, black) and the fluorescent current of the second site, $\bar I_{\rm fl}$ (dashed line, blue) together with the total fluorescent current, $\bar I_{\rm flT}$ (dot-dashed, red), divided by the donor energy $E_2 = \bar E$, are shown in Figure 3 in units of 1/ns, as functions of $\bar n$. One finds from this figure that $\bar I_{\rm en}$ and $\bar I_{\rm fl}$ currents reach saturation already for a very small $\bar n$, where less than one

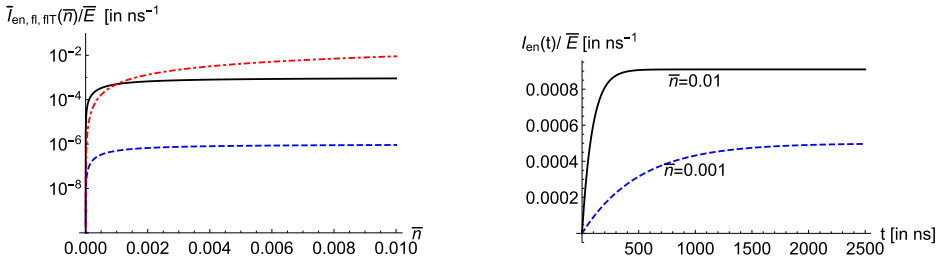

Fig. 3. Left: the steady-state energy current $\bar{I}_{\rm en}$ (solid, black) and fluorescent current $\bar{I}_{\rm fl}$ (dashed, blue) together with total fluorescent current (dot-dashed, red). Right: time-dependent energy current transferred to the RC for $\bar{n} = 0.01$ (solid line, black) and $\bar{n} = 0.001$ (dashed line, blue).

photon is absorbed at the first site during one cycle ($\tau = 1/\gamma_R = \mu$s). In addition, the fluorescent current $\bar{I}_{\rm fl}$, equation (12), is found to be very small, in comparison with the energy current, $\bar{I}_{\rm en}$, equation (11). This can be easily understood by taking into account that the energy current is the charge separation current. Indeed, it follows from equations (10d,10f) that $\gamma_R(\bar{\sigma}_{33} + \bar{\sigma}_{55}) = \Gamma(\bar{\sigma}_{22} + \bar{\sigma}_{44})$. Since the fluorescent current, $\bar{I}_{\rm fl}$, comes from the donor site (E_2), where the charge separation takes place, it proceeds with the rate Γ, which by a factor 1000 is larger than that the fluorescence rate from this site (γ). However, the total fluorescent current, $\bar{I}_{\rm flT}$, equation (12), which includes photon emission from the first site, is much larger than $\bar{I}_{\rm fl}$, and exceeds the energy current with increase of the light intensity $\bar{n}$.

One also finds from the same figure (right panel) that time for approaching the asymptotic limit increases when the intensity of light ($\bar{n}$) decreases. It is interesting that for the light intensity $\bar{n} = 0.001$ (one photon absorbed per a cycle), the current does not reach its steady-state value during the cycle, $t = \tau = 1\mu$s.

In this paper, we restrict our consideration by calculating explicitly both the energy (exciton) current and the fluorescent current, for different values of parameters. A more detailed analysis of our results, including on the ET efficiency in the LHC, in the regime of the cyclic exciton dynamics, will be presented in a separate paper.

5 Vibrational modes and noise

The role of vibrational modes in the exciton transport attracted recently much attention. It is now expected that discrete sets of strongly coupled modes can considerably enhance the transport properties along the antenna (see [12] and references therein). The reason is that the near-resonant vibrations may effectively align the electron levels. We therefore consider only one vibrational state for each site, thus truncating the Hilbert space of vibrations by two states, E_m and $E_m + \Omega$, where the vibrational frequency, Ω, is assumed to be the same for all sites. All other vibrations are considered as a part of the environment, generating fluctuations between the two states of each site (cf. with Ref. [12]). This implies that the exciton transport along the antenna can be viewed as taking place through the time-dependent energy levels of the sites, $E_m \to E_m(t) = E_m + (\Omega/2)[1 + \xi_m(t)]$ in equation (8), where $\xi_m(t) = \pm 1$ is jumping randomly from 1 to -1 (or from -1 to 1) at a rate λ_+ (or λ_-), independently of its previous history. This represents so-called dichotomic or "telegraph noise", used in many models for fluctuating environment [13–15].

If the noise is generated by a heat bath of temperature T (see for instance, Ref. [13]), then $\lambda_+/\lambda_- = \tilde{\mathcal{P}}_-/\tilde{\mathcal{P}}_+ = \exp[\Omega/(k_B T)]$, where $\tilde{\mathcal{P}}_\pm$ are probabilities for

finding $\xi_m(t)$ at the values $\xi_m = \pm 1$, $(\bar{\mathcal{P}}_+ + \bar{\mathcal{P}}_- = 1)$. The average value of $\xi_m(t)$ in the steady-state limit is therefore

$$\bar{\xi} = \langle \xi_m(t) \rangle = \sum_{\xi=\pm 1} \bar{\mathcal{P}}_\xi \xi = (\lambda_- - \lambda_+)/\lambda = \left(1 - e^{\frac{\Omega}{k_B T}}\right)/\left(1 + e^{\frac{\Omega}{k_B T}}\right). \tag{13}$$

Thus, $\bar{\xi} = 0$ for $T = \infty$, and $\bar{\xi} = -1$ for $T = 0$.

Now we exemplify our procedure for the case of two-side antenna, considered in previous section. Let us average the density matrix, $\sigma_{\alpha\alpha'}(t)$ directly in equations (10), where $E_{1,2}$ in equation (10g) are replaced by $E_{1,2} + (\Omega/2)[1 + \xi_{1,2}(t)]$. One finds that equations (10a)–(10f) keep the same form for the average density matrix $\langle \sigma_{\alpha\alpha'}(t) \rangle$. The effect of noise and vibrational modes explicitly appears only in equation (10g) via a new term $\langle \sigma_{12\xi_{1,2}} \rangle \equiv \langle \xi_{1,2}(t)\sigma_{12}(t) \rangle$. This equation now reads,

$$\langle \dot{\sigma}_{12} \rangle = i\epsilon \langle \sigma_{12} \rangle + i(\Omega/2)(\langle \sigma_{12\xi_2} \rangle - \langle \sigma_{12\xi_1} \rangle) + iV_1(\langle \sigma_{11} \rangle - \langle \sigma_{22} \rangle) - (\Gamma_T/2)\langle \sigma_{12} \rangle \tag{14}$$

where $\epsilon = E_2 - E_1$. We consider the non-correlated noise acting on different sites, where $\langle \xi_1 \xi_2 \rangle = \bar{\xi}^2$, equation (13).

In order to evaluate the second term in the r.h.s. of equation (14), we multiply each of equations (10) by $\xi_{1,2}(t)$, taking into account that $\xi^2_{1,2}(t) = 1$. For instance, multiplying equation (10g) by $\xi_2(t)$, we find,

$$\langle \xi_2 \dot{\sigma}_{12} \rangle = i\epsilon \langle \sigma_{12\xi_2} \rangle + i\frac{\Omega}{2}(1 - \bar{\xi}^2)\langle \sigma_{12} \rangle + iV_1(\langle \sigma_{11\xi_2} \rangle - \langle \sigma_{22\xi_2} \rangle) - \frac{\Gamma_T}{2}\langle \sigma_{12\xi_2} \rangle. \tag{15}$$

This equation is still not useful, since its l.h.s. is not the time-derivative of $\langle \sigma_{11\xi_2} \rangle$. However, in the case of an exponential noise-correlator, $\langle \xi(t_1)\xi(t_1 + \tau) \rangle \propto \exp(-\lambda\tau)$, one can use the following very useful "differential formula", derived by Shapiro and Loginov [16,17],

$$\frac{d}{dt}\langle \xi(t) R[\xi(t), t] \rangle = \langle \xi(t) \frac{d}{dt} R[\xi(t), t] \rangle - \lambda \langle \xi(t) R[\xi(t), t] \rangle + \lambda \bar{\xi} R[\xi(t), t], \tag{16}$$

where $\bar{\xi}$ is given by equation (13) and $R[\xi(t), t]$ is an arbitrary functional of the noise. In our case $R[\xi(t), t] \equiv \sigma_{12}(t)$, obtained from equation (10g) with the time-dependent energy levels, $E_2 - E_1 \to \epsilon + (\Omega/2)[\xi_2(t) - \xi_1(t)]$. Substituting equation (16) into equation (15) we find,

$$\begin{aligned} \langle \dot{\sigma}_{12\xi_2} \rangle = i\Big(\epsilon + i\frac{\Gamma_T + 2\gamma}{2}\Big)\langle \sigma_{12\xi_2} \rangle + \Big[\lambda\bar{\xi} + i\frac{\Omega}{2}(1 - \bar{\xi}^2)\Big]\langle \sigma_{12} \rangle \\ + iV_1\big(\langle \sigma_{11\xi_2} \rangle - \langle \sigma_{22\xi_2} \rangle\big)\langle \sigma_{12\xi_2} \rangle. \end{aligned} \tag{17}$$

Similar results are obtained for equations (10a)–(10f), by applying the differential formula (16). By proceeding in the same way with equations (10), multiplied by the random variable $\xi_1(t)$, we finally obtain the closed set of the linear equations, describing the density matrix $\sigma_{\alpha\alpha'}(t)$, giving the energy and fluorescent currents, equations (11), (12).

Consider the steady-state limit, $\bar{\sigma}_{\alpha\alpha'} = \langle \sigma_{\alpha\alpha'}(t \to \infty) \rangle$, where the l.h.s. of equations (10) vanishes. Then, these equations with the account of equation (14) become algebraic for variables $\bar{\sigma}_{\alpha\alpha'}$ and $\bar{\sigma}_{12\xi_{1,2}} \equiv \langle \xi_{1,2}(t)\sigma_{12}(t) \rangle_{t\to\infty}$. The latter terms are obtained from Eqs. (10), multiplied by $\xi_{1,2}(t)$ in the limit $t \to \infty$. For instance, these

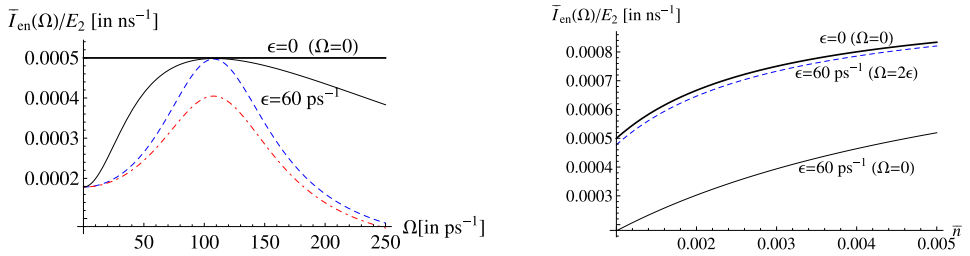

Fig. 4. Energy current in 2-site antenna in the presence and without vibrations and noise.

equations for $\bar{\sigma}_{12\xi_1}$ become,

$$\bar{\sigma}_{00\xi_1} + \bar{\sigma}_{11\xi_1} + \bar{\sigma}_{22\xi_1} + \bar{\sigma}_{33\xi_1} + \bar{\sigma}_{44\xi_1} + \bar{\sigma}_{55\xi_1} = \bar{\xi}, \tag{18a}$$

$$iV_1(\bar{\sigma}_{12\xi_1} - \bar{\sigma}_{21\xi_1}) - \Gamma_{\rm out}\bar{\sigma}_{11\xi_1} + \Gamma_{\rm in}\bar{\sigma}_{00\xi_1} + \gamma\,\bar{\sigma}_{44\xi_1} + \gamma_R\bar{\sigma}_{55\xi_1} - \lambda\bar{\sigma}_{11\xi_1} + \lambda\bar{\xi}\bar{\sigma}_{11} = 0\,, \tag{18b}$$

$$iV_1(\bar{\sigma}_{21\xi_1} - \bar{\sigma}_{12\xi_1}) - (\gamma + \Gamma + \Gamma_{\rm in})\bar{\sigma}_{22\xi_1} + \Gamma_{\rm out}\bar{\sigma}_{44\xi_1} - \lambda\bar{\sigma}_{22\xi_1} + \lambda\bar{\xi}\bar{\sigma}_{22} = 0, \tag{18c}$$

$$-(\Gamma_{\rm in} + \gamma_R)\bar{\sigma}_{33\xi_1} + \Gamma_{\rm out}\bar{\sigma}_{55\xi_1} + \Gamma\bar{\sigma}_{22\xi_1} - \lambda\bar{\sigma}_{33\xi_1} + \lambda\bar{\xi}\bar{\sigma}_{33} = 0, \tag{18d}$$

$$(\gamma + \Gamma_{\rm out} + \Gamma)\bar{\sigma}_{44\xi_1} + \Gamma_{\rm in}\bar{\sigma}_{22\xi_1} - \lambda\bar{\sigma}_{44\xi_1} + \lambda\bar{\xi}\bar{\sigma}_{44} = 0, \tag{18e}$$

$$-(\Gamma_{\rm out} + \gamma_R)\bar{\sigma}_{55\xi_1} + \Gamma_{\rm in}\bar{\sigma}_{33\xi_1} + \Gamma\bar{\sigma}_{44\xi_1} - \lambda\bar{\sigma}_{55\xi_1} + \lambda\bar{\xi}\bar{\sigma}_{55} = 0, \tag{18f}$$

$$i\Big(\epsilon + i\frac{\Gamma_T}{2}\Big)\bar{\sigma}_{12\xi_1} + \big[\lambda\bar{\xi} - i\frac{\Omega}{2}(1 - \bar{\xi}^2)\big]\bar{\sigma}_{12} + iV_1(\bar{\sigma}_{11\xi_1} - \bar{\sigma}_{22\xi_1}) = 0\,, \tag{18g}$$

where equation (18a) is obtained from the probability conservation. Respectively, equations for $\bar{\sigma}_{12\xi_2}$ are the same with a replacement $\xi_1 \to \xi_2$ and $\Omega \to -\Omega$ in equation (18g). By solving these equations, we can find the steady-state currents in the system, equations (11), (12).

An example of such calculations is presented in Figure 4. Left panel presents steady-state energy current, $I_{\rm en}/E_2$, as a function of the vibration frequency, Ω, for misaligned levels ($\epsilon = 60\,{\rm ps}^{-1}$) and the light intensity $\bar{n} = 0.001$, corresponding to one photon absorbed by the first site per a cycle (1 μs). Three curves correspond to different values of the noise-spectrum width: $\lambda = 0.001,\ 0.1,\ 10\,{\rm ps}^{-1}$ (dot-dashed red, dashed blue and solid (thin) lines, respectively). The noise is taken at room temperature. For a comparison, thick solid line (black) shows the result for aligned levels, but without vibrations and noise. We should point out that the effect of noise disappears in the limit $\lambda \to 0$ and also for $\lambda \to \infty$ (not shown here).

Right panel shows the energy current as a function of the light intensity for misaligned levels without the noise and vibrations (thin solid line black) and with the noise at the resonance ($\Omega = 2\epsilon$, dashed line blue). Thick solid line (black) displays the result for aligned levels without the noise. The results shown in Figure 4 demonstrate that incoherent fluctuations between vibronic levels can greatly increase the energy current without stringent resonance condition.

6 Summary

Although most investigations of energy (exciton) transport in the LHCs concentrate on one-exciton motion along the antenna, without inclusion of a very slow cyclic dynamics, we demonstrated that it is not sufficient for a consistent description of

exciton dynamics. Therefore, we extended the Hamiltonian by including additional parts, describing the exciton creation and the fluorescence, through the interaction with the electromagnetic field, charge separation on the donor site, and the charge restoration after completing the corresponding cycle of the chemical reactions in the RC. The latter part is described phenomenologically, as an electron relaxation from the RC to the donor's ground state by emission of fictitious bosons, representing the energy transfer to the RC.

Since our cycled master equations represent a more detailed description of the LHC dynamics, one can evaluate important effects, which cannot be treated by other methods. For instance, despite a very rapid exciton transfer along the antenna, $\sim$ps, a very slow cyclic dynamics strongly affects the exciton current. This is unavoidable, since the current does not reach its steady value during a cycle. Moreover, the slow cycle dynamics enhances very drastically the loss of exciton due to fluorescence (taking place on the scale of $\sim$ns). The reason is that the excitons are trapped during the cycle, and even one exciton trapping decreases the energy current very strongly. The multi-exciton trapping, appearing at stronger light intensity, increases the fluorescent current furthermore. These states can also be relevant for artificial photosynthetic systems.

The influence of vibrational structures on exciton transport in LHC attracted considerable attention last years. Indeed, near-resonance under-damped vibrations can considerably enhance transport properties. This assumes, however, a fine adjustment between coherent vibration frequency and a mismatch between the energy levels of neighboring sites, carrying the exciton current. In this work, we considered a different approach, where interaction with the thermal environment turns the coherent vibrations into incoherent fluctuations between the vibronic levels. As a result, the exciton transport along the antenna can be described by the (time-dependent) tunneling Hamiltonian, where the energy levels of each site are under the dichotomic (telegraph) noise, which is in the thermal equilibrium with the environment. We demonstrated here that the dichotomic noise can be treated exactly, without additional complications of the equations of motion.

This work was carried out under the auspices of the National Nuclear Security Administration of the U.S. Department of Energy at Los Alamos National Laboratory under Contract No. DE-AC52-06NA25396. R.T.S. acknowledges support from the LDRD program at LANL. S.G. is thankful to the CNLS of LANL for its hospitality and for a financial support of his visit, where a part of this work was done.

Author contribution statement

S.G. contributed in developing a mathematical approach and an illustrative material. G.P.B. contributed in modeling the LHC-RC system and in estimation of required parameters. D.T.S. contributed in adjusting parameters to the experimentally available.

References

1. M. Mohseni, Y. Omar, G.S. Engel, M.B. Plenio (Eds.), *Quantum Effects in Biology* (Cambridge University Press, Cambridge, 2014)
2. F. Caycedo-Soler, F.J. Rodríguez, L. Quiroga, Phys. Rev. Lett. **104**, 158302 (2010)
3. B. Brüggemann, V. May, J. Chem. Phys. **118**, 746 (2003)
4. D. Abramavicius, S. Mukamel, J. Chem. Phys. **133**, 064510 (2010)

5. S.A. Gurvitz, Ya.S. Prager, Phys. Rev. B **53**, 15932 (1996)
6. S.A. Gurvitz, Phys. Rev. B **56**, 15215 (1997)
7. S.A. Gurvitz, Phys. Rev. B **57**, 6602 (1998)
8. S. Gurvitz, Front. Phys. **12**, 120303 (2017)
9. D.F. Walls, G.J. Milburn, *Quantum Optics* (Springer-Verlag, Berlin, Heidelberg, 2008)
10. U. Weiss, *Quantum Dissipative Systems* (World Scientific, Singapore, 1993)
11. G. Lindblad, Commun. Math. Phys. **48**, 119 (1976)
12. N. Killoran, S.F. Huelga, M.B. Plenio, J. Chem. Phys. **143**, 155102 (2015)
13. J. Bergli, Y.M. Galperin, B.L. Altshuler, New J. Phys. **11**, 025002 (2009)
14. A. Aharony, S. Gurvitz, O. Entin-Wohlman, S. Dattagupta, Phys. Rev. B **82**, 245417 (2010)
15. S. Gurvitz, A.I. Nesterov, G.P. Berman, J. Phys. A: Math. Theor. **50**, 365601 (2017)
16. V.E. Shapiro, V.M. Loginov, Physica A **91**, 563 (1978)
17. S. Gurvitz, A. Aharony, O. Entin-Wohlman, Phys. Rev. B **94**, 075437 (2016)